Bremsstrahlung in electron-ion Coulomb scattering in strongly coupled plasma using the hyperbolic-orbit trajectory method

Young-Dae Jung
Department of Physics, Hanyang University, Ansan, Kyunggi-Do 425-791, South Korea

Hwan-Don Jeong
Department of Physics, Hanyang University, Seoul 133-791, South Korea

(Received 11 January 1996)

Classical bremsstrahlung in electron-ion Coulomb scattering in strongly coupled plasmas is investigated using the classical curved trajectory method. In strongly coupled plasmas, the electron-ion interaction potential is obtained by the ion-sphere model potential. The modified hyperbolic-orbit trajectory method is applied to describe the motion of the projectile electron in order to investigate the variation of the differential bremsstrahlung radiation cross section as a function of the impact parameter and ion-sphere radius. The results show that the scaled doubly differential bremsstrahlung radiation cross sections have minima at the small impact parameter region for soft photon radiation. For hard photon radiation, the minima disappear. The impact parameter corresponding to the minimum position of the bremsstrahlung radiation cross section recedes from the center of the ion core as the ion-sphere radius increases. The radiation cross section is substantially reduced as the radiation energy increases, especially for the large ion-sphere radius. [S1063-651X(96)12007-9]

PACS number(s): 52.20.−j, 31.15.Gy, 52.25.Tx

I. INTRODUCTION

Electron-ion Coulomb bremsstrahlung [1–11] has received much attention since this process has wide applications in many areas of physics, such as the modeling of laboratory fusion [7] and astrophysical plasmas [4], as well as in basic research in astrophysics [4,6], atomic physics [1–3,10], and plasma physics [5,7–9,11]. Recently, the bremsstrahlung in collisions of electrons with ions in high-temperature plasmas has been of great interest since the continuum bremsstrahlung radiation spectrum can also be used for plasma diagnostics [7,8]. There have been many investigations for the bremsstrahlung processes in plasmas using both quantum mechanical [1,4,5,7,8] and classical [2,3,6,9–11] methods. It has been known that the classical trajectory method [2,6,9–11] can visualize the atomic transition probabilities as a function of the impact parameter. Hence, the classical straight-line (SL) and hyperbolic-orbit (HO) trajectory methods [4,12,13] have been widely used to investigate the electron-ion collisional excitation and bremsstrahlung processes. Recently, in strongly coupled plasmas, the bremsstrahlung processes have been investigated using the SL trajectory method [11]. However, in strongly coupled plasmas, the bremsstrahlung processes have not been investigated using the curved trajectory method. In dense plasmas, an individual electron-ion encounter is influenced by the interactions of the surrounding electrons. The Coulomb interactions in strongly coupled plasmas cannot be described by the Debye-Hückel model because of the large plasma coupling parameter. A description of the strongly coupled plasmas is provided by the ion-sphere model [15,16]. Astrophysical dense plasmas are those we find in the interiors, surfaces, and outer envelopes of astronomical objects, such as neutron stars, white dwarfs, the Sun, etc. The states of plasmas for the inertial confinement fusion research are quite similar to the those of the solar interior. In these circumstances of the strongly coupled plasmas, the curved trajectory method is more reasonable to describe the motion of the projectile electron rather than the straight-line trajectory. Thus, in this paper we investigate the bremsstrahlung processes in strongly coupled plasmas using the classical modified HO trajectory method with the ion-sphere model potential. The results show that the scaled doubly differential bremsstrahlung radiation (SDDBR) cross sections have minima at the small impact parameter region for soft photon radiation. These minima have not been found using the straight-line trajectory method [2,6,9]. For hard photon radiation, the minima disappeared. The impact parameter corresponding to the minimum position of the bremsstrahlung radiation cross section recedes from the center of the ion core as the ion-sphere radius increases. The radiation cross section is substantially reduced as the radiation energy increases, especially, for the large ion-sphere radius.

In Sec. II, we derive the classical expression of the bremsstrahlung cross section in Coulomb scattering of nonrelativistic electrons with ions in strongly coupled plasmas described by the ion-sphere model potential using the HO trajectory method. Here, we introduce the modification on the impact parameter. In Sec. III, we obtain the scaled doubly differential bremsstrahlung radiation cross section as a function of the impact parameter and ion-sphere radius. We also investigate the variation of the bremsstrahlung radiation cross section with a change of the impact parameter, ion-sphere radius, and radiation photon energy. Finally, in Sec. IV, a summary and discussion are given.

II. CLASSICAL BREMSSTRAHLUNG CROSS SECTION

The classical expression of the bremsstrahlung cross section [2] is given by

$$d\sigma_b = 2\pi \int db\ b\ dw_\omega(b), \tag{1}$$

where b is the impact parameter and dw_ω is the differential probability of emitting a photon of frequency within $d\omega$ when an electron projectile changes its velocity in a collision with a static target system. For all impact parameters, the differential probability dw_ω is obtained by the Larmor formula [3] for the emission spectrum of a nonrelativistic accelerated electron,

$$dw_\omega = \frac{8\pi e^2}{3\hbar c^3} |\mathbf{a}_\omega|^2 \frac{d\omega}{\omega}, \tag{2}$$

where $\mathbf{a}_\omega$ is the Fourier coefficient of the acceleration of the projectile electron $\mathbf{a}(t)$ of the time variable t,

$$\mathbf{a}_\omega = \frac{1}{2\pi} \int_{-\infty}^{\infty} dt\ e^{i\omega t}\mathbf{a}(t). \tag{3}$$

To compute $\mathbf{a}_\omega$ we can set up coordinate axes so that the electron orbit is in the x-y plane; then

$$|\mathbf{a}_\omega|^2 = \frac{1}{m} (|F_{x\omega}|^2 + |F_{y\omega}|^2), \tag{4}$$

where $F_{x\omega}$ and $F_{y\omega}$ are the x and y components of the Fourier coefficients of the Coulomb force $\mathbf{F}(t)$ between the projectile electron and the target system:

$$F_{\mu\omega} = \frac{1}{2\pi} \int_{-\infty}^{\infty} dt\ e^{i\omega t} F_\mu(t) \quad (\mu = x,y). \tag{5}$$

In strongly coupled plasmas the Coulomb interaction potential between the projectile electron and the target ion with charge Z can be represented by the ion-sphere model [15,16],

$$V(\mathbf{r}) = -\frac{Ze^2}{r}\left[1 - \frac{r}{2R_Z}\left(3 - \frac{r^2}{R_Z^2}\right)\right]\theta(R_Z - r), \tag{6}$$

where $\mathbf{r}$ is the position vector of the projectile electron from the center of the target ion and $\theta(z)$ ($=1$ if $z \geqslant 0$;$=0$ if $z<0$) is the step function. This ion-sphere model is expected to be reasonable for low temperature and high density; i.e., where ions are frozen into a lattice. Presumably, at high temperature and density, when the potential energy is large compared to the kinetic energy, the model is also reasonable. Here R_Z is the ion-sphere radius (or called the Wigner-Seitz radius) and is given by the plasma electron density n_e,

$$R_Z = \left(\frac{3Z}{4\pi n_e}\right)^{1/3}, \tag{7}$$

since the total charge within the sphere is neutral. We now neglect electron-electron interactions altogether due to the cancellation of their radiation fields [2]. Then, the corresponding force is given by

$$\mathbf{F}(\mathbf{r}) = -Ze^2\mathbf{r}\left(\frac{1}{r^3} - \frac{1}{R_Z^3}\right)\theta(R_Z - r). \tag{8}$$

For an electron projectile, the convenient parametric representation [12,13] of the HO trajectory for $\mathbf{r}(t)$ in x-y plane is

$$x = d(\epsilon^2 - 1)^{1/2}\sinh w,$$

$$y = d(-\cosh w + \epsilon),$$

$$r(t) \equiv |\mathbf{r}(t)| = d(\epsilon \cosh w - 1),$$

$$t = \frac{d}{v}(\epsilon \sinh w - w), \quad -\infty < w < \infty, \tag{9}$$

where d, $\epsilon(=1+b^2/d^2)^{1/2}$, and v are half of the distance of closest approach in a head-on collision, the eccentricity, and the initial velocity of the projectile electron, respectively. Including the plasma-screening effects, the parameter d is obtained by a simple perturbational calculation with the ion-sphere potential [Eq. (6)]:

$$d = \left(\frac{1}{d_0} + \frac{3}{2R_Z}\right)^{-1}, \tag{10}$$

where $d_0 \equiv Ze^2/mv^2$, since $d/R_Z < 1$. After some straightforward manipulation, the Fourier coefficients of the force are found to be

$$F_{\mu\omega} = -\frac{Ze^2}{\pi \bar{v} \bar{a}_Z^2} \bar{F}_{\mu\omega}, \quad (\mu = x,y), \tag{11}$$

where $a_Z(=a_0/Z)$ is the first Bohr radius of hydrogenic ion with nuclear charge Z and $\bar{v} \equiv v/a_Z$. The Fourier coefficients $\bar{F}_{x\omega}$ and $\bar{F}_{y\omega}$ are, respectively,

$$\bar{F}_{x\omega} = \frac{1}{2}\int_{-w_Z}^{w_Z} dw \left[\frac{1}{\bar{d}(\epsilon \cosh w - 1)^2} - \frac{\bar{d}^2(\epsilon \cosh w - 1)}{\bar{R}_Z^3}\right] \times (\epsilon^2 - 1)^{1/2} \sinh w e^{i\gamma(\epsilon \sinh w - w)}, \tag{12}$$

$$\bar{F}_{y\omega} = \frac{1}{2}\int_{-w_Z}^{w_Z} dw \left[\frac{1}{\bar{d}(\epsilon \cosh w - 1)^2} - \frac{\bar{d}^2(\epsilon \cosh w - 1)}{\bar{R}_Z^3}\right] \times (-\cosh w + \epsilon) e^{i\gamma(\epsilon \sinh w - w)}, \tag{13}$$

where $\bar{d} \equiv d/a_Z$, $\bar{R}_Z \equiv R_Z/a_Z$, and $\gamma \equiv \omega d/v$. Here, the upper bound of the integral w_Z has been obtained by the interaction range ($r \leqslant R_Z$) of the ion-sphere potential [Eq. (6)] and $r(t)$ in Eq. (9):

$$W_Z=\ln\left\{\frac{\left(\frac{\overline{R_Z}}{\overline{d_0}}+\frac{5}{2}\right)}{\left[1+\left(\frac{1}{\overline{d_0}}+\frac{3}{2\overline{R_Z}}\right)^2\overline{b^2}\right]^{1/2}}+\left[\frac{\left(\frac{\overline{R_Z}}{\overline{d_0}}+\frac{5}{2}\right)^2}{\left[1+\left(\frac{1}{\overline{d_0}}+\frac{3}{2\overline{R_Z}}\right)^2\overline{b^2}\right]^{1/2}}-1\right]^{1/2}\right\}, \quad (14)$$

where $\overline{d_0}\equiv d_0/a_Z$. We now discuss the modification on the impact parameter. From Eq. (14), the upper bound of b is found to be greater than $\overline{R_Z}$. However, this is physically unreasonable since the interaction potential vanishes for $r>R_Z$. Hence, the trajectory of the projectile electron for $b>R_Z$ would be a SL one. The modified HO trajectory would be then the HO trajectory for $|w|\leqslant w_Z$ and the SL trajectory for $|w|>w_Z$. Here w_Z can be obtained by Eq. (9), $R_Z=d(\epsilon\cosh w_Z-1)$. From Eq. (9), the tangent at the point $(x_Z[\equiv x(w_Z)],y_Z[\equiv y(w_Z)])$ becomes

$$y=-\frac{\tanh w_Z}{(\epsilon^2-1)^{1/2}}x+d(-\cosh w_Z+\epsilon)+d\sinh w_Z\tanh w_Z. \quad (15)$$

The modified impact parameter b' can be obtained by the perpendicular distance from the origin to this tangent,

$$b'=\frac{d(\epsilon^2-1)^{1/2}\cosh w_Z(-\cosh w_Z+\epsilon)+d(\epsilon^2-1)^{1/2}\sinh^2 w_Z}{[\sinh^2 w_Z+(\epsilon^2-1)\cosh^2 w_Z]^{1/2}} \quad (16a)$$

$$=d(\epsilon^2-1)^{1/2}\left(\frac{\epsilon\cosh w_Z-1}{\epsilon\cosh w_Z+1}\right)^{1/2}. \quad (16b)$$

After some algebra, the relationship between the general scaled impact parameter $\bar{b}(\equiv b/a_Z)$ and the modified scaled impact parameter $\overline{b'}(\equiv b'/a_Z)$ becomes

$$\bar{b}=\overline{b'}\left(\frac{\tilde{E}+\frac{7}{2\overline{R_Z}}}{\tilde{E}+\frac{3}{2\overline{R_Z}}}\right)^{1/2}, \quad (17)$$

where $\tilde{E}(\equiv mv^2/2Z^2\mathrm{Ry})$ is the scaled energy of the projectile electron. Then, in the nonrelativistic limit the classical bremsstrahlung cross section can be obtained by Eqs. (1), (12), and (17);

$$d\sigma_b=\frac{16}{3}\frac{\alpha a_0^2}{\tilde{E}}\frac{d\omega}{\omega}\int_{\overline{b'_{\min}}}^{\overline{b'_{\max}}}\overline{b'}\,d\overline{b'}(|\overline{F_{x\omega}}|^2+|\overline{F_{y\omega}}|^2), \quad (18)$$

where $\alpha(=e^2/\hbar c\approx\frac{1}{137})$ is the fine structure constant. Here, the modified minimum scaled impact parameter $\overline{b'_{\min}}$ corresponds to the closest distance of approach at which the ion-sphere potential energy of interaction is equal to the maximum possible energy transfer,

$$2mv^2=\frac{Ze^2}{b'}\left[1-\frac{b'}{2R_Z}\left(3-\frac{b'^2}{R_Z^2}\right)\right]. \quad (19)$$

Then, it is found that $\overline{b'_{\min}}\cong(2\tilde{E}+3/2\overline{R_Z})^{-1}$. The modified maximum scaled impact parameter $\overline{b'_{\max}}$ is determined by Eqs. (7) and (14); $\overline{b'_{\max}}=\overline{R_Z}$.

III. BREMSSTRAHLUNG RADIATION CROSS SECTION

The differential bremsstrahlung radiation cross section [3] is defined by

$$\frac{d\chi_b}{d\varepsilon}\equiv\frac{d\sigma_b}{\hbar d\omega}\hbar\omega \quad (20a)$$

$$=\frac{16}{3}\frac{\alpha a_0^2}{E}\int_{\overline{b'_{\min}}}^{\overline{R_Z}}\overline{b'}\,d\overline{b'}(|\overline{F_{x\omega}}|^2+|\overline{F_{y\omega}}|^2), \quad (20b)$$

where $\varepsilon(\equiv\hbar\omega)$ is the energy of the radiation photon. In the nonrelativistic limit, the parameter γ can be expressed as

$$\gamma=\frac{\tilde{\epsilon}}{2\sqrt{\tilde{E}}\left(\tilde{E}+\frac{3}{2\overline{R_Z}}\right)}, \quad (21)$$

where $\tilde{\varepsilon}(\equiv\hbar\omega/Z^2\mathrm{Ry})$ is the scaled energy of the radiation photon. Then the scaled doubly-differential bremsstrahlung radiation (SDDBR) cross section obtained by the modified HO trajectory, i.e., the differential bremsstrahlung radiation cross section per unit scaled impact parameter, becomes

$$\left(\frac{d^2\chi_b}{d\tilde{\epsilon}\, d\overline{b'}}\right)_{\rm HO} \Big/ \pi a_0^2 = \frac{16}{3\pi}\frac{\alpha^3}{\tilde{E}}\frac{\tilde{b}'}{\left(\tilde{E}+\dfrac{3}{2R_Z}\right)}\left\{\left|\int_{-w_Z}^{w_Z}\frac{dw}{2}\frac{\tilde{b}'\sinh w}{\left(\tilde{E}+\dfrac{3}{2R_Z}\right)}\left[\frac{\left(\tilde{E}+\dfrac{3}{2R_Z}\right)^2}{[(1+\tilde{b}'^2)^{1/2}\cosh w-1]}\right.\right.\right.$$

$$\left.\left.-\frac{(1+\tilde{b}'^2)^{1/2}\cosh w-1}{\left(\tilde{E}+\dfrac{3}{2R_Z}\right)\overline{R_Z^3}}\right]\exp\left[i\frac{\tilde{\varepsilon}[(1+\tilde{b}'^2)^{1/2}\sinh w-w]}{2\sqrt{\tilde{E}}\left(\tilde{E}+\dfrac{3}{2R_Z}\right)}\right]\right|^2$$

$$+\left|\int_{-w_Z}^{w_Z}\frac{dw}{2}[-\cosh w+(1+\tilde{b}'^2)^{1/2}]\left[\frac{\left(\tilde{E}+\dfrac{3}{2R_Z}\right)}{[(1+\tilde{b}'^2)^{1/2}\cosh w-1]}\right.\right.$$

$$\left.\left.\left.-\frac{(1+\tilde{b}'^2)^{1/2}\cosh w-1}{\left(\tilde{E}+\dfrac{3}{2R_Z}\right)^2\overline{R_Z^3}}\right]\exp\left[i\frac{\tilde{\varepsilon}[(1+\tilde{b}'^2)^{1/2}\sinh w-w]}{2\sqrt{\tilde{E}}\left(\tilde{E}+\dfrac{3}{2R_Z}\right)}\right]\right|^2\right\}, \qquad (22)$$

where the modified interval w_Z is given by

$$w_Z=\ln\left\{\frac{\left(\tilde{E}+\dfrac{5}{2\overline{R_Z}}\right)\overline{R_Z}}{(1+\tilde{b}'^2)^{1/2}}+\left[\frac{\left(\tilde{E}+\dfrac{5}{2\overline{R_Z}}\right)^2\overline{R_Z^2}}{(1+\tilde{b}'^2)}-1\right]^{1/2}\right\}, \qquad (23)$$

with $\tilde{b}'\equiv[(\tilde{E}+3/2\overline{R_Z})(\tilde{E}+7/2\overline{R_Z})]^{1/2}\overline{b'}$. The dependence of the SDDBR cross section on the plasma-screening effects has been explicitly indicated through the scaled ion-sphere radius R_Z. This SDDBR cross section is dimensionless since all physical parameters are normalized.

In order to investigate the plasma-screening effects, we consider the three cases of the ion-sphere radius: $\overline{R_Z}=10$, 20, and 40. We also consider the two cases of the ratio of the radiation photon energy to the projectile electron energy: $\tilde{\varepsilon}/\tilde{E}(=\varepsilon/E)=0.1$ (the soft radiation photon) and 0.5 (the hard radiation photon). Here, we choose that $\tilde{E}=0.2$, i.e., $E=0.2Z^2$Ry, since the classical trajectory method is known to be reliable for low-energy projectiles ($v<Z\alpha c$) [2]. Table I shows the numerical values of the SDDBR cross sections at $\overline{b'}=5\overline{R_Z}/3$ for the three cases of the ion-sphere radius: $\overline{R_Z}=10$, 20, and 40 when $\tilde{E}=0.2$. The SDDBR cross sections are substantially decreased with increasing the radiation photon energy, especially for the large ion-sphere radius (e.g., $\cong$0.8% for $\overline{R_Z}=10$, $\cong$16.5% for $\overline{R_Z}=20$, and $\cong$79.3% for $\overline{R_Z}=40$). However, for the small ion-sphere radius, the SDDBR cross sections are almost unchanged with varying the radiation photon energy. The SDDBR cross sections are illustrated in Fig. 1, where the full curve is that for $\tilde{\varepsilon}/\tilde{E}=0.1$ and the dotted curve that for $\tilde{\varepsilon}/\tilde{E}=0.5$. The radiation cross sections are terminated at the corresponding ion-sphere radii since $\overline{b'}\leq\overline{R_Z}$. As we can see in Fig. 1, the SDDBR cross sections have minima at small-impact parameter region for soft photon radiation. For hard photon radiation, the minima have been disappeared. The minimum position of the SDDBR cross section recedes from the center of the ion core as the ion-sphere radius increases. Since the SDDBR cross section corresponds to the differential radiation probability, the minimum represents the minimum probability. The SL trajectory method can be obtained by changing the parameters as $x=vt$ and $y=b'$ in Eq. (9). We can also verify that

$$\left(\frac{d^2\chi_b}{d\tilde{\varepsilon}\, d\overline{b'}}\right)_{\rm SL}=\lim_{\substack{\overline{d}\to 0\\ \overline{\gamma}\to 0\\ \overline{\varepsilon\, d}\to \overline{b'}}}\left(\frac{d^2\chi_b}{d\tilde{\varepsilon}\, d\overline{b'}}\right)_{\rm HO}. \qquad (24)$$

Figure 2 shows the SDDBR cross sections obtained by the SL trajectory method. The SDDBR cross sections are substantially decreased with increasing the radiation photon energy, especially at the large ion-sphere radius ($\overline{R_Z}=40$). For small-impact parameters the SL trajectory method is not quite reliable since the SL method is the classical analog of the Born approximation [17]. As we see in Figs. 1 and 2, the SDDBR cross sections obtained by the modified HO trajec-

TABLE I. Numerical values of the scaled doubly differential bremsstrahlung radiation cross sections obtained by the modified HO trajectory method [Eq. (22)] at $\overline{b'}=5\overline{R_Z}/3$ for the three cases of the ion-sphere radius: $\overline{R_Z}=10$, 20, and 40 when $\tilde{E}=0.2$.

$\tilde{\varepsilon}/\tilde{E}$	$\left(\frac{d^2\chi_b(\overline{b'}=5\overline{R_Z}/3)}{d\tilde{\varepsilon}\, d\overline{b'}}\right)_{\rm HO}\Big/\pi a_0^2$ $\overline{R_Z}=10$	$\overline{R_Z}=20$	$\overline{R_Z}=40$
0.1	1.3803×10^{-6}	1.9940×10^{-6}	3.2206×10^{-6}
0.5	1.3688×10^{-6}	1.6655×10^{-6}	6.6634×10^{-7}

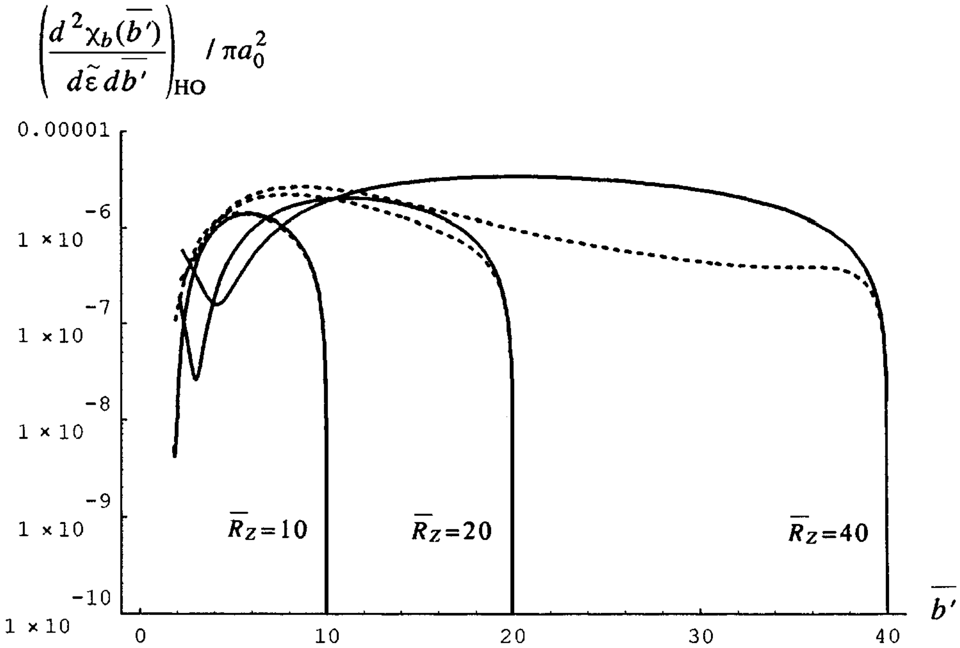

FIG. 1. The scaled doubly differential bremsstrahlung radiation cross sections obtained by the modified HO trajectory method for the three cases of the ion-sphere radius: $\bar{R}_Z=10$, 20, and 40 when $\tilde{E}=0.2$. The full curve represents Eq. (22) for $\tilde{\varepsilon}/\tilde{E}=0.1$. The dotted curve represents Eq. (22) for $\tilde{\varepsilon}/\tilde{E}=0.5$.

tory method and by the SL trajectory method are quite different. The minimum phenomena cannot be found in the SL trajectory method [11]. Because of the strong Coulomb effects within the ion-sphere ($\bar{b}'\leqslant\bar{R}_Z$), the modified HO curved trajectory method is more reliable than the SL trajectory method in the classical approximation.

IV. SUMMARY AND DISCUSSIONS

We investigate the plasma-screening effects for the bremsstrahlung in electron-ion Coulomb scattering in-strongly coupled plasmas using the classical hyperbolic-orbit trajectory method. In strongly coupled plasmas the electron-ion interaction potential is obtained by the ion-sphere model potential. The hyperbolic-orbit trajectory method is applied to describe the motion of the projectile electron in order to investigate the variation of the scaled doubly differential bremsstrahlung radiation cross section as a function of the impact parameter and ion-sphere radius. The results show that the scaled doubly differential bremsstrahlung radiation cross sections have minima at the small impact parameter region for soft photon radiations. These minima have not been found using the straight-line trajectory method. For hard photon radiations, the minima disappeared. The impact parameter corresponding to the minimum position of the radiation cross section recedes from the center of the ion core as the ion-sphere radius increases. The radiation cross section is substantially reduced as the radiation photon energy increases, especially, for the large ion-sphere radius. These results provide a general description of the classical bremsstrahlung processes in electron-ion Coulomb scattering in strongly coupled plasmas.

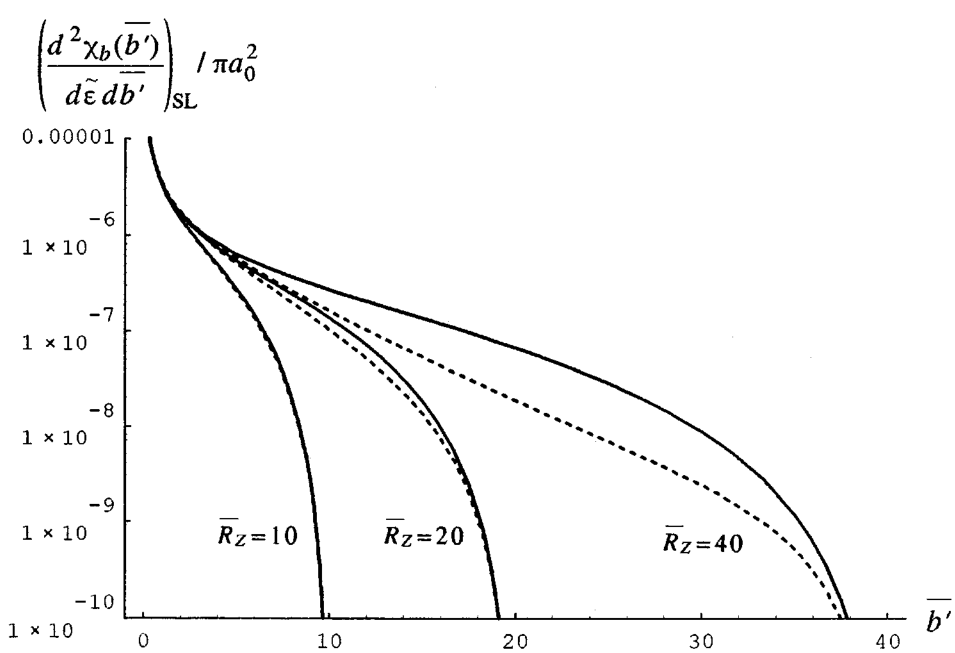

FIG. 2. The scaled doubly differential bremsstrahlung radiation cross sections obtained by the SL trajectory method for the three cases of the ion-sphere radius: $\bar{R}_Z=10$, 20, and 40 when $\tilde{E}=0.2$. The full curve represents Eq. (24) for $\tilde{\varepsilon}/\tilde{E}=0.1$. The dotted curve represents Eq. (24) for $\tilde{\varepsilon}/\tilde{E}=0.5$.

ACKNOWLEDGMENTS

One of the authors (Y.-D. Jung) thanks Professor R. J. Gould for useful comments and interesting discussions. This research was supported in part by the Korea Science and Engineering Foundation through Grant No. 961-0205-021-2, by the Korea Basic Science Institute through the HANBIT User Development Program (FY1996), and by the Korea Ministry of Education through the Basic Science Research Institute Program (BSRI-96-2448).

[1] H. A. Bethe and E. E. Salpeter, *Quantum Mechanics of One- and Two-Electron Atoms* (Academic, New York, 1957).
[2] R. J. Gould, Am. J. Phys. **38**, 189 (1970).
[3] J. D. Jackson, *Classical Electrodynamics*, 2nd ed. (Wiley, New York, 1975).
[4] R. J. Gould, Astrophys. J. **238**, 1026 (1980); **243**, 677(E) (1981).
[5] H. Totsuju, Phys. Rev. A **32**, 3005 (1985).
[6] M. S. Longair, *High Energy Astrophysics*, 2nd ed. (Cambridge University Press, Cambridge, 1992).
[7] K. E. Voss and N. J. Fisch, Phys. Fluids B **4**, 762 (1992); **5**, 659(E) (1993).
[8] Y.-D. Jung, Phys. Plasmas **1**, 788 (1994).
[9] G. Bekefi, *Radiation Processes in Plasmas* (Wiley, New York, 1966).
[10] L. D. Landau and E. M. Lifshitz, *The Classical Theory of Fields*, 4th ed. (Pergamon, Oxford, 1975).
[11] Y.-D. Jung, Phys. Plasmas **3**, 1741 (1996).
[12] L. D. Landau and E. M. Lifshitz, *Mechanics*, 3rd ed. (Pergamon, Oxford, 1976).
[13] Y.-D. Jung, Astrophys. J. **409**, 841 (1993).
[14] Y.-D. Jung and I.-D. Cho, Phys. Rev. E **52**, 5333 (1995).
[15] E. E. Salpeter, Austr. J. Phys. **7**, 373 (1954).
[16] Y.-D. Jung, Phys. Plasmas **2**, 1775 (1995).
[17] F. H. Shu, *The Physics of Astrophysics, Vol. 1 Radiation* (University Science Books, Mill Valley, CA, 1991).